Research Square

Preprints are preliminary reports that have not undergone peer review.
They should not be considered conclusive, used to inform clinical practice,
or referenced by the media as validated information.

Chemical-diffusion Metamaterials with “Plug and Switch” Modules for Ion Cloaking, Concentrating and Selection: Design and Experiments

Yang Li
University of Science and Technology Beijing
Chengye Yu
University of Science and Technology Beijing
Chuanbao Liu
University of Science and Technology Beijing
Zhengjiao Xu
University of Science and Technology Beijing
Yan jing Su
Beijing Advanced Innovation Center for Materials Genome Engineering, University of Science and Technology Beijing https://orcid.org/0000-0003-2773-4015
Lijie Qiao
University of Science and Technology Beijing
Ji Zhou
Tsinghua University
Yang Bai (baiy@mater.ustb.edu.cn)
University of Science and Technology Beijing https://orcid.org/0000-0002-6917-256X

Article

Keywords: metamaterials, "plug and switch", physical fields, chemical diffusion

Posted Date: May 17th, 2021

DOI: https://doi.org/10.21203/rs.3.rs-466840/v1

License: This work is licensed under a Creative Commons Attribution 4.0 International License.
Read Full License

Chemical-diffusion Metamaterials with "Plug and Switch" Modules for Ion Cloaking, Concentrating and Selection: Design and Experiments

*Yang Li, Chengye Yu, Chuanbao Liu, Zhengjiao Xu, Yanjing Su, Lijie Qiao, Ji Zhou, and Yang Bai**

Y. Li, C. Yu, Z. Xu, Prof. Y. Su, Prof. L. Qiao, Prof. Y. Bai
Beijing Advanced Innovation Center for Materials Genome Engineering
Institute for Advanced Materials and Technology
University of Science and Technology Beijing
Beijing 100083, China
E-mail: baiy@mater.ustb.edu.cn (Y. Bai)

Dr. C. Liu
School of Materials Science and Engineering
University of Science and Technology Beijing
Beijing 100083, China

Prof. J. Zhou
State Key Laboratory of New Ceramics and Fine Processing
School of Materials Science and Engineering
Tsinghua University
Beijing 100084, China

Correspondence and requests for materials should be addressed to Y.Bai.

Abstract

The outstanding abilities of metamaterials to manipulate physical fields have been extensively studied in wave-based fields. Recently, this research has been extended to diffusion fields. Chemical diffusion behavior is crucial in a wide range of fields including the transportation of various matters, and metamaterials with the ability to manipulate diffusion with practical applications associated with chemical and biochemical engineering have not yet been proposed. In this work, we propose the idea of a “plug and switch” metamaterial to achieve the switchable functions of ion cloaking, concentrating and selection in liquid solvents by plugging modularized functional units into a functional motherboard. The respective modules are theoretically designed based on scattering cancellation, and the properties are verified by both simulations and experiments. Plugging in any module barely affects the environmental diffusion field, but the module choice impacts different diffusion behaviors in the central region. Cloaking strictly hinds ion diffusion, and concentrating promotes a large diffusion flux, while cytomembrane-like ion selection permits the entrance of some ions but blocks others. In addition to property characterization, these functions are demonstrated in special applications. The concentrating function is experimentally verified by catalytic enhancement, and the ion selection function is verified by protein protection. This work not only demonstrates the effective manipulation of metamaterials in terms of chemical diffusion behavior but also shows that the "plug and switch" design is extensible and multifunctional, and facilitates novel applications including sustained drug release, catalytic enhancement, bioinspired cytomembranes, etc.

Introduction

Metamaterials have become the hottest topic in this century because of their exotic electromagnetic properties not found in naturally occurring materials. These properties originate from the outstanding ability of metamaterials to manipulate the physical fields. In particular, the idea of an invisibility cloak, which can render an object invisible to observers, has attracted significant attention. It controls the path of electromagnetic wave transport to achieve invisibility through an inhomogeneous medium artificially designed by the theories of transformation optics[1] (TO) by Pendry and scattering cancellation[2] (SC) by Engheta. In addition to the ideal cloaking proposed by theory and demonstrated by experiments, the design is further extended to metamaterials with diversified functions such as concentrators[3,4], rotators[5,6] and illusion metamaterials[7,8]. After great success in manipulating electromagnetic waves[9-11], TO and SC were also proven to be powerful tools to manipulate not only other wave-based fields like acoustic waves[12-14] and water waves[15,16] but also diffusion fields such as thermal flux[17-25], electric fields[26-29], magnetic fields[30-34], diffusive light[35-37] and chemical fields[38-43]. For comparison, metamaterials designed by TO usually exhibit substantial inhomogeneity and anisotropy, while SC provides a simpler way to achieve cloaking for diffusion fields by obeying the Laplacian equation, i.e., Laplacian fields.

As a fundamental phenomenon in nature, chemical diffusion is a spontaneous behavior that depends on the concentration gradient and follows the Laplacian equation, i.e., a typical Laplacian field. For years, researchers have devoted their efforts to seeking a more effective method to control the behavior of diffusion for applications in chemical and biological engineering. Although the idea of manipulating chemical flow by metamaterials has been proposed for years[40,41], related research is still rare[38-43]. In particular, most studies are limited to theoretical design and numerical simulation rather than experiments, and those that do involve experimentation deal only with the tractable solid samples instead of the more general liquid environments. Additionally, the proposed chemical-diffusion metamaterials are limited to a single role, cloak or concentrator, and they have never been connected to practical applications. Compared to metamaterials used in electromagnetic fields and thermal fields that

have seen massive advances, chemical diffusion metamaterials are still prototypes and need great improvements.

As metamaterials are different from traditional materials, the key feature of cloaking and concentrating by metamaterials is to realize the minimum and maximum concentration gradient in a certain region while not altering the environmental concentration distribution. This feature is crucial to prevent specific objects from being detected through concentration variation in some chemical and biological applications. To achieve cloaking and concentrating, tailored anisotropic parameters (specifically, the diffusion coefficient) are required, which are proposed to be resolved by various passive and active components. Although the solid host is much easier to model and simulate, the extremely low diffusion efficiency is not appropriate for practical applications of chemical engineering and bioengineering, including ion separation, bioinspired devices, and drug delivery. In this work, we design chemical diffusion metamaterials with different functions for manipulating ion diffusion in liquids, including a bilayer cloak based on the SC theory, a concentrator with a fan-shaped structure and an ion selector. In addition, we propose the idea of "plug and switch" in a metamaterial device, in which different functions are switchable by plugging modularized functional units into the same motherboard without affecting the environmental concentration, as illustrated in Fig. 1. Furthermore, the designed functions are experimentally demonstrated in special applications of catalytic enhancement and protein protection that will benefit catalytic engineering and bioengineering.

Results

The experimental setup contains a functional motherboard with optimized diffusivity and some pluggable modules to switch the function of metamaterials, as shown in Fig. 1. In this work, Modules 1, 2, and 3 represent the cloak, concentrator and ion selector, respectively. They have identical geometric configurations of a 3 cm annulus with a 1 cm concentric annulus and can be plugged into the center of the same motherboard. The proposed idea of "plug and switch" with modularization design can achieve minimum perturbation to the concentration distribution in the motherboard after plugging in any module and switch the device to functions such as cloaking, concentrating, ion selection and other possible applications.

First, we design a bilayer cloak based on SC theory rather than TO theory to avoid complex anisotropic parameters. A diffusion process without convection can be expressed according to Fick's second law:

$$\frac{\partial C}{\partial t} = \nabla\left(D\nabla C\right) \tag{1}$$

where t is time, C is the mass concentration (mol m^{-3}), D is the diffusion coefficient ($m^2 \cdot s^{-1}$), and $\nabla = \frac{\partial}{\partial x}\vec{i} + \frac{\partial}{\partial y}\vec{j} + \frac{\partial}{\partial z}\vec{k}$ is the operator in the Cartesian coordinate system. In a stable state without particle sources, the concentration distribution follows the equation $\nabla^2 C = 0$. For a sphere with a radius of R_1 enclosed by a bilayer spherical cloak with an inner radius of R_2 and an outer radius of R_3, the concentration distribution in this sphere is expressed by:

$$C_1 = -\sum_{l=0}^{\infty} A_l r^l P_l\left(\cos\theta\right) \quad \left(r \le R_1\right) \tag{2}$$

where $P_l\left(\cos\theta\right)$ is a first-order Legendre polynomial and A_l is an undetermined constant. Similarly, we have the concentration distribution for the bilayer cloak:

$$\begin{aligned} C_2 &= -\sum_{l=0}^{\infty}\left[B_l r^l + D_l r^{-(l+1)}\right]P_l\left(\cos\theta\right) \quad \left(R_1 < r \le R_2\right) \\ C_3 &= -\sum_{l=0}^{\infty}\left[E_l r^l + F_l r^{-(l+1)}\right]P_l\left(\cos\theta\right) \quad \left(R_2 < r \le R_3\right) \\ C_4 &= -\sum_{l=0}^{\infty}\left[G_l r^l + H_l r^{-(l+1)}\right]P_l\left(\cos\theta\right) \quad \left(r > R_3\right) \end{aligned} \tag{3}$$

Because if $r \to 0$, then C_1 is limited and if $r \to \infty$, then $C_4 = -c_0 r\cos\theta$, and if we have continuous conditions at boundaries, we have parameters for the bilayer cloak:

$$D = \frac{2R_2^3 + R_1^3}{2\left(R_2^3 - R_1^3\right)} D_0 \tag{4}$$

For the two-dimensional case (corresponding to the bilayer annulus):

$$D = \frac{R_2^2 + R_1^2}{R_2^2 - R_1^2} D_0 \tag{5}$$

It is concluded that a bilayer cloak requires an inner layer with an index of zero and a complementary outer layer with an index associated with the background media according to Equation (4) or (5).

For a 2D chemical diffusion cloak, we use a 3D printed resin annulus (functional unit 1) to realize the zero index, which leaves only the diffusivities of the outer layer of cloak and the background media to be engineered. Then, we use the effective medium theory (EMT) to match the diffusivity of the outer layer of the cloak with that of the background media. The radii of the inner layer and the outer layer are set to 2 cm and 3 cm, respectively. The outer layer is pure water, and the internal layer is a 2 mm annulus made of resin. Therefore, the diffusivity ratio of the outer layer of the cloak and the background media is calculated as 13/5 according to Equation (5). Similar to the calculations in thermal physics, we expand the Bruggeman approximation of EMT to acquire specific diffusivity. For a two-phase system composed of water and homogeneously distributed resin pillars, the effective diffusivity is obtained as:

$$\begin{aligned} & f_1 \frac{D_1 - D_e}{2D_e + D_1} + f_2 \frac{D_2 - D_e}{2D_e + D_2} = 0 \\ & f_1 + f_2 = 1 \end{aligned} \tag{6}$$

where f_1 and f_2 are the volume ratios of water and resin pillars, D_1 and D_2 are the diffusivities of water and resin pillars and D_e is the effective diffusivity of the two-phase system. The calculated f_2 is 16/39. The difference in ion diffusivity of the two phases is on the scale of several orders of magnitude, so the ion diffusivity in resin pillars can be considered zero when the filling ratio of resin is small. In addition, we evaluate the dependence of the effective diffusivity on the filling ratio, as shown in Supplementary Fig. 1a. The approximation holds true when the effective diffusivity is high, while the effective diffusivity is linearly related to the filling ratio. However, if the effective diffusivity is close to zero, the ion diffusivity in resin pillars cannot be neglected. The optimal parameters for the functional motherboard are shown in Supplementary Fig. 1b.

The concentration distribution for the metamaterial device is simulated and shown in Fig. 2. The concentration distribution exhibits straight streamlines in a homogeneous medium, while it is clearly scattered when a circular area is removed. The undisturbed concentration distribution outside the cloak is restored when the cloaking module is plugged in and the concentration inside the cloak is nearly zero, as shown in Fig. 2c. The chemical flux is guided around the central region in the cloak and maintains a uniform distribution outside the cloak. This behavior indicates that the central region is chemically invisible to observers and that ion

shielding is achieved. We also compare the ideal cloak of homogeneous diffusivity with that of inhomogeneous diffusivity designed by EMT through simulation, as shown in Supplementary Fig. 2. To characterize the concentration contour, we measured the concentration distribution along a line y=-3.5 cm close to the cloak, which is shown in Fig. 2c. The concentration distributions at line y=-3.5 cm in these two scenarios are close, while the error is mainly because the equivalent parameters of EMT require random distribution of micro/nanoparticles in the two-phase system.

To experimentally verify the cloaking effect, we selected $CuSO_4$ solution as an example due to its distinguishing color and added the $CuSO_4$ solution and deionized water to the left and right tanks in the metamaterial device. After waiting 5 min for the solution to reach a steady state, we took samples of the solution from points inside (A) and outside (B) the cloak and along a line behind the cloak and measured the concentrations by a spectrophotometer. The concentration $\boldsymbol{c}$ is characterized by absorbance as follows:

$$\mathrm{A}(\lambda) = \alpha(\lambda) \cdot c \cdot l \tag{7}$$

where $\mathrm{A}(\lambda)$ is the absorbance, $\alpha(\lambda)$ is the absorption coefficient and l is the thickness of the sample. Since $\alpha(\lambda)$ and l are constants for a given solution with the same solute, the concentration is linearly related to the measured absorbance. The measured absorbances of points A and B are shown in Fig. 2d. The concentration of the cupric cation inside the cloak is found to be zero; this region inside the cloak benefits from the isolated conditions provided by Module 1. In addition, we take 300 μL of solution from 7 evenly spaced spots along the line at y =-3.5 cm and measure the absorbance, as shown in Supplementary Fig. 3. The measured results indicate that the scattering of the chemical gradient is drastically reduced, similar to the simulated results, as shown in Fig. 2e. That is, chemical cloaking is achieved. The detailed results of the absorbance measurements are shown in Supplementary Fig. 4. The measured results may represent the average concentration around the pipette because of deviations in the sampling point location. To determine the possible error, we also simulate the concentration distribution astride the line y =-3.5 cm, i.e., along line y =-3.45 cm and y=-3.55 cm, as shown in Supplementary Fig. 5. We notice that the concentration distribution has intense scattering

when close to resin pillars, which may cause test error during the sampling of the solution. The perturbations of concentration along lines y =-3.45 cm and y=-3.55 cm cancel each other out on average.

Second, an ion concentrator is designed in a typical fan structure as Module 2, where the invisibility is achieved by minimum perturbation when $D'_r D'_\theta = D_0^2$. Similar to the solutions in the thermal concentrator, we set $D'_r = 2^n D_0, D'_\theta = 2^{-n} D_0$. To create a concentrator, D'_r ? D'_θ is required, which indicates that the general ion diffusion is towards the radial direction and that the anisotropy determines the concentration efficiency $\frac{C_E - C_F}{C_C - C_D}$. Based on the EMT of $D'_r = D_A f_A + D_B f_B, D'_\theta = 1/\left(f_A / D_A + f_B / D_B\right)$, we chose water and resin as materials A and B, respectively. Then, the exact integration of cloaking and concentrator in the modularized metamaterials should fulfil the following condition:

$$D = \frac{R_2^2 + R_1^2}{R_2^2 - R_1^2} \sqrt{D'_r D'_\theta} \qquad (8)$$

As an intractable point of this design, an accurate measure of the diffusivity of cupric cations in resin is unknown and is also affected by many factors, including concentration and temperature. These factors make it difficult to match the diffusivity to satisfy $D'_r D'_\theta = D_0^2$, so we focus on the concentrating feature more than the invisibility feature in the design. The fraction of resin is 20% in the whole volume of Module 2, so that the diffusivity of D'_r decreases to be approximately 80% of that in pure water and D'_θ to be 0. The simulated concentration distribution for the metamaterial device with the concentrator module demonstrates that although the parameters do not strictly obey the formula, the scattering is significantly reduced compared to the blank reference, and a significantly concentrated gradient is developed in the central region, as shown in Fig. 2f. The measured concentration along the line at y= -3.5 cm in Fig. 2e is almost identical to the simulated results.

Previous studies were always limited to model design and property characterization but ignored connecting the obtained function to practical applications. Here, we use the functions

of cloaking and concentrating in some practical applications, i.e., catalytic boost and protein protection. The concentrating feature of Module 2 significantly increases the concentration gradient in the central region, which can be used to promote catalytic efficiency. We select the typical Fenton reagent as an example, which is widely used in chemical engineering to remove refractory organic pollutants. As a strong oxidation system composed of Fe^{2+} and H_2O_2, the Fenton reagent generates hydroxyl radicals and superoxide radicals with extremely strong oxidization through a chain reaction:

$$Fe^{2+} + H_2O_2 \rightarrow Fe^{3+} + HOg + OH^-$$
$$Fe^{3+} + H_2O_2 \rightarrow Fe^{2+} + HOOg + H^+$$
$$2H_2O_2 \rightarrow HOg + HOOg + H_2O$$

Although the mechanism of the above redox cycle reaction is unclear due to the complicated intermediate products, most researchers have suggested that hydroxyl groups are the origin of intense oxidation of the Fenton reagent and that Fe^{2+} serves as a catalyst, as shown in Fig. 3a. Here, the above chain reaction is simply treated as the disproportionation of hydrogen peroxide. We plug Module 2 into the motherboard and inject $FeSO_4$ solution and deionized water into the two tanks. The concentrations in the central region with and without Module 2 are measured, and a 150% increase in the concentration of Fe^{2+} is found at t = 120 s. We take the solution inside and outside the concentrator every 30 s to evaluate the concentration change with time, as shown in Fig. 3b. At every measured timepoint, the concentration inside the concentrator is obviously higher than that outside. The reduction in concentration outside of the concentrator is because the solution concentration is more susceptible to being disturbed by sampling as it approaches equilibrium.

To evaluate the catalytic efficiency of the Fenton reaction in dye degradation, we add the Fe^{2+} solution taken from inside the concentrator into the precursor solution of Fenton reagent with organic dye (Specimen 1) and add the solution from outside the concentrator to another precursor solution (Specimen 2). In addition, Specimen 3 was made by adding the deionized water to precursor solution as a blank control. The comparison of the degradation effect for different specimens is shown in Fig. 3c, and all of the results are shown in Supplementary Fig. 6. The blank control indicates that organic dye cannot be degraded by pure water. The organic dye is completely degraded after 6 min in Specimen 1, while it takes approximately 36 min to

fully degrade in Specimen 2. This result indicates that the catalytic efficiency is 6 times higher when the metamaterial device is used. The experimental results prove that the concentrator greatly promotes catalytic applications, which can be further extended to built-in metamaterials for catalytic enhancement.

The previously discussed cloak and concentrator modules remarkably change the field distribution in the central region but do not disturb the surrounding field, so they do not destroy the environmental field distribution and avoid detection through field fluctuations when they work. However, the process becomes much more complex for chemical diffusion metamaterials because diffusion may involve a variety of ions. This is a problem not faced by electromagnetic or other metamaterials. Similar to leukocytes, which detect viruses or bacteria through antigenic determinants, chemical diffusion metamaterials have the important ability to screen and selectively manipulate different ions. Here, we design the third module for our metamaterial device, a bioinspired cytomembrane-like ion selector. It enables specific ion penetration or shielding and maintains acid-base equilibrium.

Module 3 has a fan structure filled with an ion exchange resin. The ion-exchange resin contains sulfonic acid groups, carboxyl groups and phenol groups that exchange with high valent cations. As a result, the high-valent cations of Cu^{2+} are shielded out of the central region, but low-valent ions such as K+ and Na^{+} are still permitted. We demonstrate the design of a potassium ion channel. When the metamaterial device with an ion selection module is in the $CuSO_4/K_2SO_4$ gradient, the cation exchange resin preferentially reacts with cupric cations and allows potassium ions to achieve the separation of $CuSO_4/K_2SO_4$. The measured concentration inside and outside the module at 120 s is shown in Fig. 3d. The ion selector limits nearly all cupric cations while promoting the concentration of potassium ions. The concentration distribution along line y=-3.5 cm is also measured and shown in Supplementary Fig. 7. The overall concentration is lower than that of the cloak, concentrator and reference since the ion exchange resin absorbs major cupric cations.

As shown in Fig. 3e, when 100 g ion-exchange resin was mixed with 200 mL 13.2 g/L $CuSO_4$ solution, the concentration approached a saturation of 8.6 g/L after 2 hours. This result indicates that the ion exchange resin acts as the active component to absorb the cupric cation.

In addition, the absorption speed is fast enough to shield the cupric cation in the $CuSO_4$ gradient. Since a certain cation is selectively shielded, the metamaterial device with Module 3 can be used as a cytomembrane-like ion selector to prevent chemical harm in bioengineering. Protein protection is selected as a special application to demonstrate the function in the experiment. As shown in Fig. 3f, a dialysis bag sealed with bovine serum albumin (BSA) solution was placed in the center of the motherboard in a $CuSO_4$ gradient. BSA has a molecular weight of 66.5 kDa, while that of the dialysis bag is 12 kDa, which means that $CuSO_4$ can penetrate the dialysis bag and cause the denaturation of BSA. If Module 3 is absent, BSA is exposed to $CuSO_4$ and aggregates because of the conformational change and the loss of solubility. If Module 3 is plugged in, the BSA solution is unaltered after the same amount of time, demonstrating an excellent protein protection performance. Moreover, Module 3 can also be applied to anion shielding by filling the apparatus with anion exchange resin.

Note that although Module 1 of the cloak can also accomplish ion shielding, the strategy is quite different. The ion selector is an open system that selectively blocks some specific ions so that it provides more flexibility in complicated scenarios. Additionally, the ion selection function is limited by the saturation of the cation exchange resin. As more cation exchange resin is used, the length of time that the high-valent cations are blocked increases, but the effective diffusivity along the radial direction is smaller for other chemicals. This is because the ion exchange resin does not contribute to the diffusion of chemicals.

Discussion

In this paper, we proposed a design paradigm for a “plug and switch” metamaterial with pluggable functional units and switchable functions. The simulated and measured results indicate that the cloak can almost entirely reduce scattering, while the concentrator can greatly promote diffusive flux. The results prove that cloaking, concentrating and ion selection can be realized in an integrated functional motherboard with modularized functional units. The demonstrated “plug and switch” metamaterials are powerful for manipulating chemical diffusion behavior and facilitate novel applications with multiple extensible functions including sustained drug release, catalytic enhancement, bioinspired cytomembranes, etc. The

concentrator can greatly enhance the catalytic efficiency by promoting the concentration of catalysis, while the ion selector provides a protein protection case by prohibiting heavy metal ions; this ion selector can be considered a bioinspired cytomembrane with ion channels. The ability of bioinspired cytomembranes to open gives them potential for use in bioengineering applications such as sustained drug release and artificial organs.

Method

Fabrication of chemical-diffusion metamaterial: The functional motherboard and functional units are fabricated by LCD-based stereo lithography appearance 3D printing. The material is UV curable resin. The detailed size parameters are calculated based on effective medium theory. Each functional unit is attached to the motherboard by waterproof glue to prevent the ion in solution penetrating the cloaked region through the small gap in the bottom.

Experimental setup of cloak and concentrator: The experimental equipment has two tanks at left and right end with $CuSO_4$ solution and deionized water respectively to produce a certain concentration gradient, and then a diffusion platform with engineered diffusivity is connected to both tanks through a port sealed by dialysis membrane, which is adopted to slow the diffusion at the port and prevent convection. After the liquid is added to both tanks and the diffusion platform between the tanks, the dialysis membrane is removed slowly.

Concentration measurement: 300 μL solution is taken at each spot along line x= -4 cm by a multi-channel pipette and transfered to a labeled centrifuge tube. The solution is diluted by 3 ml water and measured the absorbance by spectrophotometer. For the concentration measurement by inductively coupled plasma, the dilution is selective depending on the concentration.

Preparation of precursor in catalytic boost demonstration: After 40 ml methyl blue with a concentration of 10 mg/L is taken and the pH is tuned to ~3 by H_2SO_4, 2 ml H_2O_2 is added in the solution and mixed by magnetic stirring to prepare the precursor solution. For the cases with and without concentrator, 300 μL solution in central region is taken and mixed with specimen 1 and 2 with 50 ml precursor solution respectively, while specimen 3 adopts 300 μL water as blank control.

Data availability

All the relevant data are available from the correspondence authors upon reasonable request.

Acknowledgements

This work was supported by grants from the National Natural Science Foundation of China (91963114), Beijing Municipal Science and Technology Project (Z191100004819002) and Major Science and Technology Programs of Yunnan (202002AB080001-1).

Supplementary information

Supporting Information is available online or from the author.

Competing interests

The authors declare no conflict of interest.

Author contributions

Y.L. and Y.B. conceptualized the initial ideas carried out simulations. Y.L. and Y.B. performed the experiments with support from C.Y and Z.X. All authors were involved in data interpretation. Y.L. prepared the initial manuscript with contribution from all the authors and Y.B. revised the manuscript.

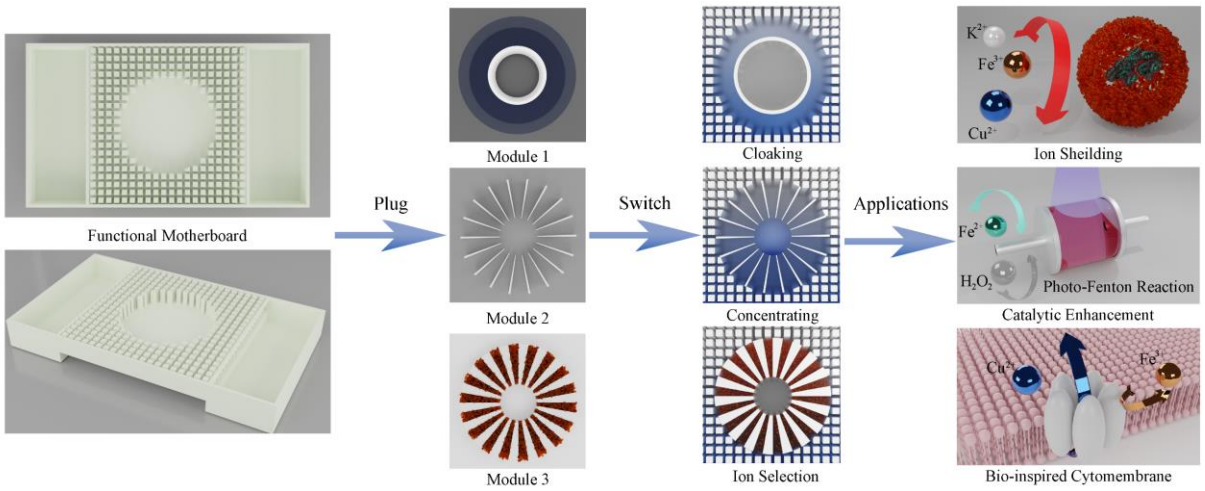

Fig.1 Conceptual illustration of "plug and switch" metamaterial. By Plugging in different modules in the functional motherboard, the chemical diffusion metamaterials can manipulate the behavior of ion diffusion to realize ion cloaking, concentrating and ion selection in liquid solvents. The modularized metamaterials with integrated ion manipulating functions can be further extended to applications like ion shielding, catalytic enhancement and bio-inspired cytomembrane.

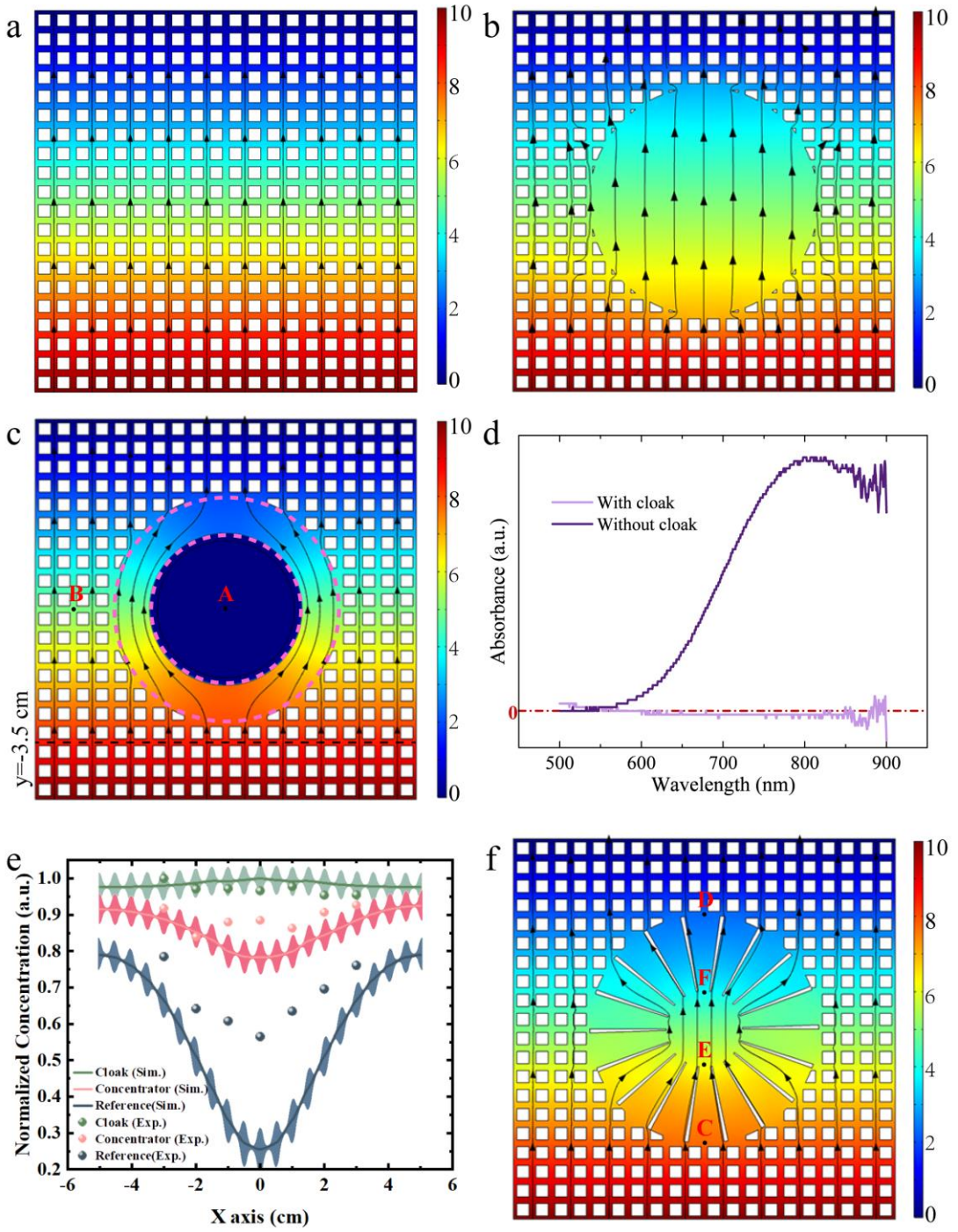

Fig. 2 Simulated and measured results of cloak and concentrator. a Simulated concentration surface and flux lines for background. **b** Simulated concentration surface and flux lines for reference. **c** Simulated concentration surface and flux lines for Cloak. **d** Measure concentration at point A with and without cloak. **e** Measure results of concentration distribution at line y= -3.5 for reference, cloak and concentrator. Error bar are plotted based on Supplementary fig. 5 to evaluate the scattering of resin pillars. **f** Simulated concentration surface and flux lines for concentrator.

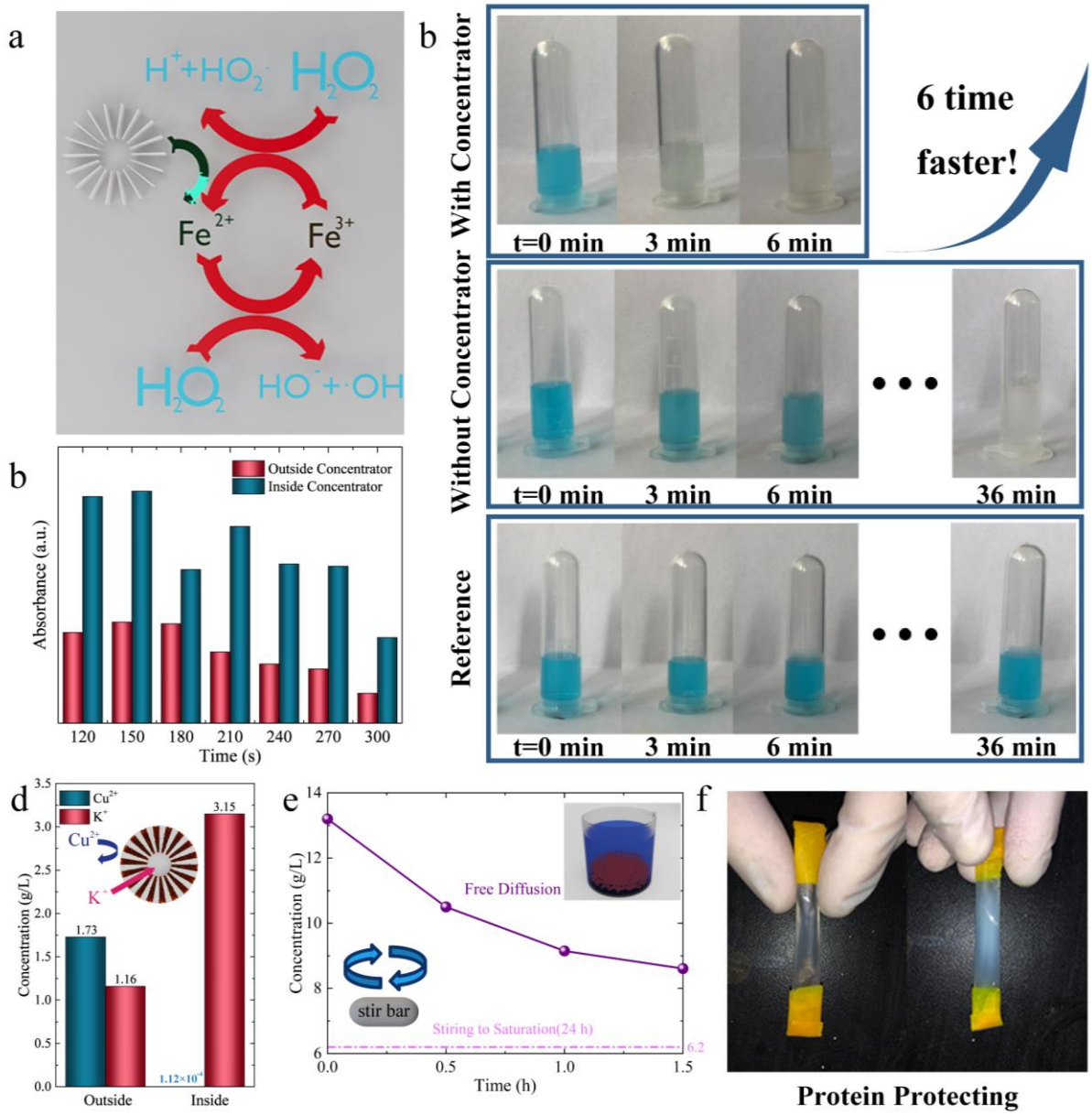

Fig. 3 Demonstration of catalytic and bioengineering applications. a Illustration of Fenton reaction boosted by concentrator. **b** Time dependent measurement of concentration inside and outside the concentrator. **c** Observation of catalytic boost by concentrator. **d** Concentration inside and outside the ion selecting metamaterials in concentration gradient of $CuSO_4/K_2SO_4$. **e** Adsorption of cupric cation by ion exchange resin. **f** Demonstration of protein protecting application by ion selecting metamaterials.

References

1 Pendry, J. B., Schurig, D. & Smith, D. R. Controlling electromagnetic fields. *Science* **312**, 1780-1782 (2006).

2 Alù, A. & Engheta, N. Achieving transparency with plasmonic and metamaterial coatings. *Phys. Rev. E* **72**, 016623 (2005).

3 Navau, C., Prat-Camps, J. & Sanchez, A. Magnetic Energy Harvesting and Concentration at a Distance by Transformation Optics. *Phys. Rev. Lett.* **109**, 263903 (2012).

4 Han, T. *et al.* Theoretical realization of an ultra-efficient thermal-energy harvesting cell made of natural materials. *Energy Environ. Sci.* **6**, 3537-3541 (2013).

5 Chen, H. *et al.* Design and Experimental Realization of a Broadband Transformation Media Field Rotator at Microwave Frequencies. *Phys. Rev. Lett.* **102**, 183903 (2009).

6 Yang, F., Tian, B., Xu, L. & Huang, J. Experimental Demonstration of Thermal Chameleonlike Rotators with Transformation-Invariant Metamaterials. *Phys. Rev. Appl.* **14**, 54024 (2020).

7 Hu, R. *et al.* Illusion Thermotics. *Adv. Mater.* **30**, 1707237.1707231-1707237.1707238 (2018).

8 Lai, Y. *et al.* Illusion Optics: The Optical Transformation of an Object into Another Object. *Phys. Rev. Lett.* **102**, 253902 (2009).

9 Schurig, D. *et al.* Metamaterial electromagnetic cloak at microwave frequencies. *Science* **314**, 977-980 (2006).

10 Liu, R. *et al.* Broadband ground-plane cloak. *Science* **323**, 366-369 (2009).

11 Ma, H. F. & Cui, T. J. Three-dimensional broadband and broad-angle transformation-optics lens. *Nat. Commun.* **1**, 1-7 (2010).

12 Zigoneanu, L., Popa, B.-I. & Cummer, S. A. Three-dimensional broadband omnidirectional acoustic ground cloak. *Nat. Mater.* **13**, 352-355 (2014).

13 Zhang, S., Xia, C. & Fang, N. Broadband acoustic cloak for ultrasound waves. *Phys. Rev. Lett.* **106**, 024301 (2011).

14 Cummer, S. A. *et al.* Scattering theory derivation of a 3D acoustic cloaking shell.

Phys. Rev. Lett. **100**, 024301 (2008).

15 Zou, S. *et al.* Broadband waveguide cloak for water waves. *Phys. Rev. Lett.* **123**, 074501 (2019).

16 Li, C. *et al.* Concentrators for water waves. *Phys. Rev. Lett.* **121**, 104501 (2018).

17 Xu, H., Shi, X., Gao, F., Sun, H. & Zhang, B. Ultrathin three-dimensional thermal cloak. *Phys. Rev. Lett.* **112**, 054301 (2014).

18 Fan, C., Gao, Y. & Huang, J. Shaped graded materials with an apparent negative thermal conductivity. *Appl. Phys. Lett.* **92**, 251907 (2008).

19 Guenneau, S., Amra, C. & Veynante, D. Transformation thermodynamics: cloaking and concentrating heat flux. *Opt. Express* **20**, 8207-8218 (2012).

20 Narayana, S. & Sato, Y. Heat flux manipulation with engineered thermal materials. *Phys. Rev. Lett.* **108**, 214303 (2012).

21 Han, T., Yuan, T., Li, B. & Qiu, C.-W. Homogeneous thermal cloak with constant conductivity and tunable heat localization. *Sci. Rep.* **3**, 1-5 (2013).

22 Schittny, R., Kadic, M., Guenneau, S. & Wegener, M. Experiments on transformation thermodynamics: molding the flow of heat. *Phys. Rev. Lett.* **110**, 195901 (2013).

23 Han, T. *et al.* Experimental demonstration of a bilayer thermal cloak. *Phys. Rev. Lett.* **112**, 054302 (2014).

24 Su, Y. *et al.* Path-Dependent Thermal Metadevice beyond Janus Functionalities. *Adv. Mater.* **33**, 2003084 (2021).

25 Li, Y. *et al.* Thermal meta-device in analogue of zero-index photonics. *Nat. Mater.* **18**, 48-54 (2019).

26 Yang, F., Mei, Z. L., Jin, T. Y. & Cui, T. J. DC electric invisibility cloak. *Phys. Rev. Lett.* **109**, 053902 (2012).

27 Han, T. *et al.* Manipulating DC currents with bilayer bulk natural materials. *Adv. Mater.* **26**, 3478-3483 (2014).

28 Yang, F., Mei, Z. L., Yang, X. Y., Jin, T. Y. & Cui, T. J. A negative conductivity material makes a dc invisibility cloak hide an object at a distance. *Adv. Funct. Mater.* **23**, 4306-4310 (2013).

29 Li, Y. *et al.* Scattering Cancellation by a Monolayer Cloak in Oxide Dispersion-Strengthened Alloys. *Adv. Funct. Mater.* **30**, 2003270 (2020).

30 Sanchez, A., Navau, C., Prat-Camps, J. & Chen, D.-X. Antimagnets: controlling magnetic fields with superconductor–metamaterial hybrids. *New J. Phys.* **13**, 093034 (2011).

31 Gömöry, F. *et al.* Experimental realization of a magnetic cloak. *Science* **335**, 1466-1468 (2012).

32 Narayana, S. & Sato, Y. DC magnetic cloak. *Adv. Mater.* **24**, 71-74 (2012).

33 Jiang, W., Ma, Y. & He, S. Static magnetic cloak without a superconductor. *Phys. Rev. Appl.* **9**, 054041 (2018).

34 Jiang, W. *et al.* Room-temperature broadband quasistatic magnetic cloak. *NPG Asia Mater.* **9**, e341-e341 (2017).

35 Schittny, R. *et al.* Invisibility cloaking in light-scattering media. *Laser Photon. Rev.* **10**, 382-408 (2016).

36 Schittny, R. *et al.* Transient behavior of invisibility cloaks for diffusive light propagation. *Optica* **2**, 84-87 (2015).

37 Schittny, R., Kadic, M., Bückmann, T. & Wegener, M. Invisibility cloaking in a diffusive light scattering medium. *Science* **345**, 427-429 (2014).

38 Li, Y., Liu, C., Bai, Y., Qiao, L. & Zhou, J. Ultrathin Hydrogen Diffusion Cloak. *Adv. Theory Simul.* **1**, 1700004 (2018).

39 Guenneau, S. & Puvirajesinghe, T. Fick's second law transformed: one path to cloaking in mass diffusion. *J. R. Soc. Interface* **10**, 20130106 (2013).

40 Guenneau, S., Petiteau, D., Zerrad, M., Amra, C. & Puvirajesinghe, T. Transformed Fourier and Fick equations for the control of heat and mass diffusion. *AIP Adv.* **5**, 053404 (2015).

41 Zeng, L. & Song, R. Controlling chloride ions diffusion in concrete. *Sci. Rep.* **3**, 1-7 (2013).

42 Restrepo-Flórez, J. M. & Maldovan, M. Mass separation by metamaterials. *Sci. Rep.* **6**, 1-8 (2016).

43 Avanzini, F., Falasco, G. & Esposito, M. Chemical cloaking. *Phys. Rev. E* **101**, 060102 (2020).

Supplementary Files

This is a list of supplementary files associated with this preprint. Click to download.

- SupplementaryInformation.docx